# Control-Augmented Structural Synthesis

R. V. Lust* and L. A. Schmit†
*University of California, Los Angeles, California*

**A control-augmented structural synthesis methodology is presented in which the structural member sizes and active control system feedback gains are treated simultaneously as independent design variables. Multiple static and harmonic dynamic loading conditions are considered. Constraints are imposed on static displacements, natural frequencies, and the magnitudes of the steady-state dynamic displacements and actuator forces to ensure acceptable system behavior. Side constraints imposed on the design variables protect against the generation of unrealizable designs. Example problems are presented that demonstrate the method and underscore the importance of integrating the structural and active control system design process.**

## Introduction

THE design of efficient structural systems is of fundamental interest to both structural and control engineers. Systematic methodologies for both structural and active control system synthesis (e.g., structural optimization and optimal control therapy) are well known and are receiving increased application in the design environment. However, for the most part, these design techniques, have been applied independently within the overall design process. Specifically, a design methodology has evolved in which the structure is designed subject to prescribed strength and stiffness requirements (while ignoring the active control system) with the active control system being subsequently designed under the assumption that the structure is prescribed.

The design challenge presented by large flexible space structures has generated interest in interdisciplinary approaches to the design problem.[1-3] This interest has been heightened as a result of both numerical and experimental demonstrations of the synergic nature of active and passive control techniques.[4-6] Consequently, several design methodologies have been proposed in the past few years.

One class of methods utilizes linear optimal control theory to unify the structure/control design process. In this approach, the optimal controls are expressed as a function of the structural design variables and a design problem is then formulated in terms of the structural variables alone.[7,8]

An alternative approach, which treats both the structural and control variables as design variables, is given in Ref. 9. In this case, the structural and active control system design problems are performed sequentially within an iteration loop and are coupled through the constraints of the structural synthesis problem.

Neither of the approaches discussed above integrates the structural and control system design problems into a single synthesis problem statement in terms of an independent set of structural and control design variables. Several other recent works[10-14] have begun to address this task. While these proposed approaches consider transient response constraints indirectly, they do not impose design constraints directly on the response quantities (e.g., dynamic displacements, actuator forces) and they do not include constraints associated with static loading conditions.

Presented as Paper 86-1014 at the AIAA/ASME/ASCE/AHS 27th Structure, Structural Dynamics and Materials Conference, San Antonio, TX, May 19–21, 1986; received July 18, 1986; revision received April 23, 1987. 

*Graduate Research Assistant (currently Senior Research Engineer, General Motors Research Laboratories, Warren, MI).

†Professor of Engineering and Applied Science. Fellow AIAA.

In this paper, a methodology for control-augmented structural synthesis is proposed for a class of structures that can be modeled as an assemblage of frame and/or truss elements. The structural sizing variables and the active control system feedback gains are treated simultaneously as independent design variables. Design constraints are imposed on static and steady-state dynamic displacements and actuator forces as well as natural frequencies. Lower-bound side constraints on the feedback gains are used to indirectly guard against dynamic instability.[15] It is assumed that both the plant (structure) and the active control system dynamics can be adequately approximated with a linear model. While the proposed approach is more general, here the methodology is developed and demonstrated for the case where: 1) the dynamic loading is harmonic and thus the steady-state response is of primary interest, 2) direct output feedback[16-18] is used for the control system model, and 3) the actuators and sensors are collocated.

## Problem Statement

For an important class of problems, the control-augmented structural synthesis problem may be stated as

$$\min_{\boldsymbol{Y}} c_1 M(\boldsymbol{Y}) + c_2 J(\boldsymbol{Y})$$
$$\text{s.t. } \boldsymbol{G}(\boldsymbol{Y}) \le 0, \qquad \boldsymbol{Y}^L \le \boldsymbol{Y} \le \boldsymbol{Y}^U \tag{1}$$

where $M$ is the structural mass, $J$ a performance index, $c_1$ and $c_2$ scalar weighting coefficients on $M$ and $J$, and $\boldsymbol{G}$ the vector of behavior constraints (e.g., constraints on static and dynamic displacements, actuator forces, and natural frequencies). The design variable vector $\boldsymbol{Y}$ includes both the structural sizing variables [e.g., frame member cross-sectional dimensions (CSD)] and the control system position and velocity feedback gains. The vectors $\boldsymbol{Y}^U$ and $\boldsymbol{Y}^L$ are the upper and lower bounds on $\boldsymbol{Y}$.

In this work, the performance index $J$ is chosen to be a weighted sum of the steady-state dynamic displacements $u$ and the actuator forces $F_A$ and is given by

$$J(\boldsymbol{Y}) = J_R(\boldsymbol{Y}) + J_C(\boldsymbol{Y}) = \sum_{k=1}^{K_d} \sum_{j \in N_R} Q_{jk} |u_{jk}(\boldsymbol{Y})| + \sum_{k=1}^{K_d} \sum_{i \in N_C} R_{ik} |F_{A_{ik}}(\boldsymbol{Y})| \tag{2}$$

where $J_R$ and $J_C$ are the portions of the performance index associated with the system response and the control force, respectively, $K_d$ the number of dynamic loading conditions, $N_R$ the set of displacements to be included in $J_R$, and $N_C$ the set of actuator forces to be included in $J_C$. The quantities $Q_{jk}$ and $R_{ik}$ are weighting coefficients on the magnitudes of the dynamic displacements and actuator forces and are set equal to the

reciprocals of the allowable values associated with constraints imposed on these quantities.[19]

The substitution of Eq. (2) into Eq. (1) will yield a complete statement of the control-augmented structual synthesis problem. While there is no conceptual difficulty in solving this problem, given specific values for $c_1$ and $c_2$, the a priori selection of appropriate values for these coefficients can be difficult. It is often necessary to solve such a problem several times with different values of $c_1$ and $c_2$ before acceptable values of $M$ and $J$ are obtained.

An alternative approach is to consider the following two special cases: 1) the case where $c_1 = 1$ and $c_2 = 0$ and 2) the case where $c_1 = 0$ and $c_2 = 1$. In the first case, the objective function is the structual mass. Two constraints are added to the problem statement to limit the maximum allowable values of $J_R$ and $J_C$ since they are no longer contained in the objective function. The resulting problem statement is

$$\begin{aligned} &\min_{\boldsymbol{Y}} M(\boldsymbol{Y}) \\ &\text{s.t. } \boldsymbol{G}(\boldsymbol{Y}) \le 0, \qquad J_R(\boldsymbol{Y}) \le J_R^U \\ &J_C(\boldsymbol{Y}) \le J_C^U, \qquad \boldsymbol{Y}^L \le \boldsymbol{Y} \le \boldsymbol{Y}^U \end{aligned} \tag{3}$$

where $J_R^U$ and $J_C^U$ are upper bounds on $J_R$ and $J_C$, respectively. It should be noted that, for many practical design problems, constraints on the dynamic displacements included in $\boldsymbol{G}$ will adequately limit the system response and, in those cases, the upper-bound constraints on $J_R$ can be removed from the problem statement.

The second case (i.e., $c_1 = 0$, $c_2 = 1$) can be further specialized to cases where $J_R$ and $J_C$ appear independently in the objective function giving

$$\begin{aligned} &\min_{\boldsymbol{Y}} J_R(\boldsymbol{Y}) \\ &\text{s.t. } \boldsymbol{G}(\boldsymbol{Y}) \le 0, \qquad M(\boldsymbol{Y}) \le M^U \\ &J_C(\boldsymbol{Y}) \le J_C^U, \qquad \boldsymbol{Y}^L \le \boldsymbol{Y} \le \boldsymbol{Y}^U \end{aligned} \tag{4}$$

where the upper-bound constraints on $M$ and $J_C$ are added to compensate for the removal of the structural mass and total control force from the objective function and

$$\begin{aligned} &\min_{\boldsymbol{Y}} J_C(\boldsymbol{Y}) \\ &\text{s.t. } \boldsymbol{G}(\boldsymbol{Y}) \le 0, \qquad M(\boldsymbol{Y}) \le M^U \\ &J_R(\boldsymbol{Y}) \le J_R^U, \qquad \boldsymbol{Y}^L \le \boldsymbol{Y} \le \boldsymbol{Y}^U \end{aligned} \tag{5}$$

where the upper-bound constraints on $M$ and $J_R$ are added to compensate for the removal of the structural mass and response measure from the objective function (although the upper-bound constraint on $J_R$ may be deleted for certain problems, as described previously).

The control augmented structural synthesis problems given in Eqs. (3–5) represent a collection of problem formulations that are applicable to the design of a significant class of structures and their associated active control systems. Each problem formulation is best applied to achieve one of the following three design objectives: 1) the minimization of structural mass [Eq. (3)], 2) the minimization of the structural response associated with selected degrees of freedom [Eq. (4)], and 3) the minimization of the total control force [Eq. (5)].

## Solution Method

The control-augmented structural synthesis problem posed in Eqs. (3–5) can, in principle, be solved via the direct application of any one of several well-known nonlinear mathematical programming algorithms. However, since both the objective and constraint functions are complicated, implicit, nonlinear functions of the design variables, this approach is computationally impractical even for small systems. A more tractable approach is to replace these implicit nonlinear mathematical programming problems with a sequence of explicit approximate problems of reduced dimensionality,[20–22] having the following form [shown here for the control force minimization problem, Eq. (5)]:

$$\begin{aligned} &\min_{\boldsymbol{Y}} \tilde{J}_C(\boldsymbol{Y}) \\ &\text{s.t. } \tilde{g}_q(\boldsymbol{Y}) \le 0, \qquad q \in Q_R \\ &\tilde{\boldsymbol{Y}}^L \le \boldsymbol{Y} \le \tilde{\boldsymbol{Y}}^U \end{aligned} \tag{6}$$

where $\tilde{J}_C$ is an explicit approximation of the control force, $\tilde{g}_q$ are explicit approximations of a subset $Q_R$ of the original set of behavior constraints (including the constraints on $M$ and $J_R$), and $\boldsymbol{Y}$ is now the vector of linked design variables. The vectors $\tilde{\boldsymbol{Y}}^U$ and $\tilde{\boldsymbol{Y}}^L$ are the stepwise upper and lower bounds on the design variables and are chosen to protect the validity of the approximations.

The solution to the actual design problem is obtained through the iterative construction and solution of a sequence of approximate problems (see Fig. 1). The generation and solution of each approximate problem consists of the following three steps: 1) analysis, 2) approximate problem generation, and 3) optimization. These steps are repeated until the design process has converged. This process is terminated when the

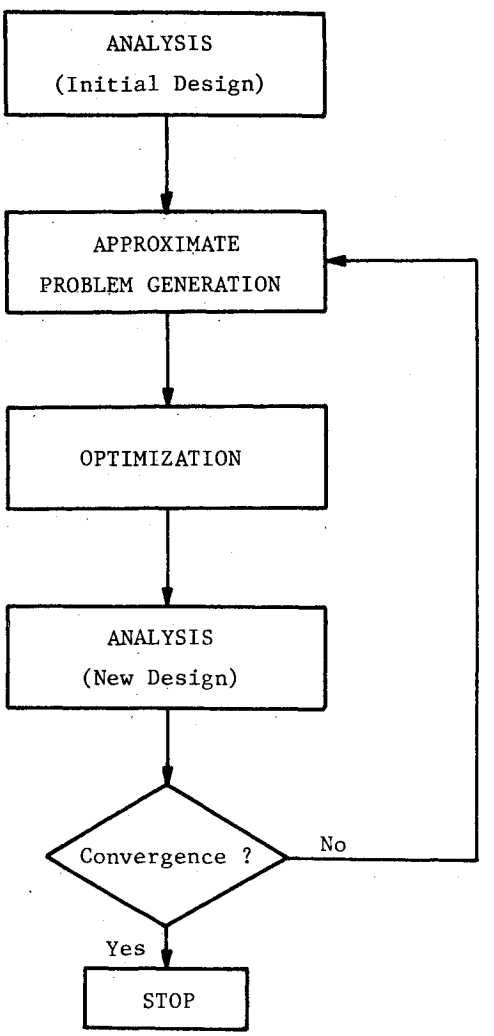


**Fig. 1 Solution method flow diagram.**

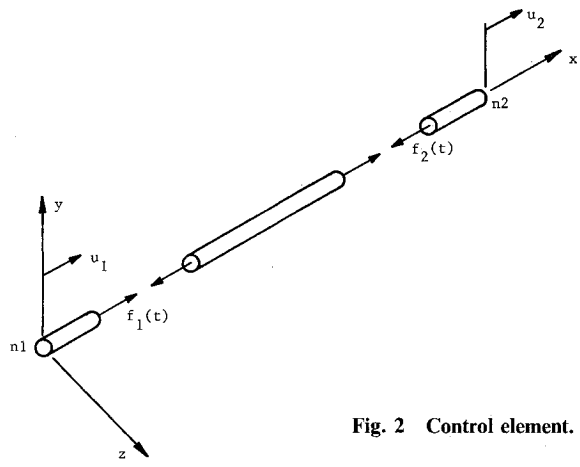


**Fig. 2 Control element.**

relative change in the objective function values for three consecutive iterations is less than a prescribed tolerance.

**Analysis**

Evaluation of both the objective and constraint functions in Eqs. (3–5) requires the analysis of the structural/control system. In this work, the discretized governing equations of motion are obtained via a finite-element displacement method formulation. For the class of problems considered here, the underlying analysis equations for multiple static loading conditions are given by

$$[K]\{u\}_k = \{P\}_k; \quad k = 1,2,\ldots,K_s \tag{7}$$

where $[K]$ is the structural stiffness matrix, $\{u\}_k$ the static displacement vectors, and $\{P\}_k$ the static load vectors. The undamped natural frequencies for the open-loop system are obtained by solving the structural dynamics eigenvalue problem

$$[K][\Phi] = [M][\Phi][\omega^2] \tag{8}$$

where $[M]$ is the structural mass matrix, $[\omega^2]$ the diagonal matrix of eigenvalues, and $[\Phi]$ the matrix of eigenvectors. For multiple dynamic loading, the equations of motion are given by

$$[M]\{\ddot{u}\}_k + [C]\{\dot{u}\}_k + [K]\{u\}_k = \{P(t)\}_k; \quad k = 1,2,\ldots,K_d \tag{9}$$

where $[C]$ is the viscous damping matrix and $\{P(t)\}_k$ the $k$th dynamic load vector. The vectors $\{u\}_k$, $\{\dot{u}\}_k$, and $\{\ddot{u}\}_k$ are the dynamic displacements, velocities, and accelerations associated with the $k$th loading condition.

Equation (9) can be augmented to include the active control forces by introducing the discretized actuator forces $\{N(t)\}_k$, giving

$$[M]\{\ddot{u}\}_k + [C]\{\dot{u}\}_k + [K]\{u\}_k = \{N(t)\}_k + \{P(t)\}_k; \quad k = 1,\ldots,K_d \tag{10}$$

Using a linear direct output feedback[16–18] control law, the actuator forces can be written in terms of the system level position and velocity feedback gain matrices $[G_p]$ and $[G_v]$ as

$$\{N(t)\}_k = -[G_v]\{\dot{u}\}_k - [G_p]\{u\}_k \tag{11}$$

Substituting Eq. (11) into Eq. (10), the closed-loop equations of motion can be written as

$$[M]\{\ddot{u}\}_k + [C_A]\{\dot{u}\}_k + [K_A]\{u\}_k = \{P(t)\}_k; \quad k = 1,\ldots,K_d \tag{12}$$

where the control augmented damping and stiffness matrices are given by

$$[C_A] = [C] + [G_v] \tag{13}$$

and

$$[K_A] = [K] + [G_p] \tag{14}$$

The system level feedback gain matrices ($[G_p]$ and $[G_v]$) are assembled from the element level gain matrices of the active control elements (see Fig. 2). Each control element represents an actuator connected between two nodes of the structural model and is similar to the member damper described in Ref. 23. The actuator exerts a force proportional to the relative displacements and velocities at the connecting nodes. The element level actuator forces can be written as

$$\begin{Bmatrix} f_1(t) \\ f_2(t) \end{Bmatrix} = -h_p \begin{bmatrix} 1 & -1 \\ -1 & 1 \end{bmatrix} \begin{Bmatrix} u_1 \\ u_2 \end{Bmatrix} - h_v \begin{bmatrix} 1 & -1 \\ -1 & 1 \end{bmatrix} \begin{Bmatrix} \dot{u}_1 \\ \dot{u}_2 \end{Bmatrix} \tag{15}$$

or

$$\{F_A\} = -[H_p]\{u\}^e - [H_v]\{\dot{u}\}^e \tag{16}$$

where $\{F_A\}$ is the control force vector, $[H_p]$ and $[H_v]$ the position and velocity feedback gain matrices, and $\{u^e\}$ and $\{\dot{u}\}^e$ the components of the dynamic displacement and velocity vectors associated with the control element.

The solution of Eqs. (7) and (8) is straightforward and, therefore, will not be elaborated upon here. For the case where the external dynamic loading is harmonic with

$$\{P(t)\}_k = \{P\}_k \sin \Omega_k t \tag{17}$$

Eq. (12) can be modified to include structural damping and its solution can be obtained by solving the following sets of linear algebraic equations for the unknowns $\{c_R\}_k$ and $\{c_I\}_k$[24]:

$$\begin{bmatrix} \Omega_k[C_A]_k + \gamma[K] & [K_A]_k - \Omega_k^2[M] \\ [K_A]_k - \Omega_k^2[M] & -\Omega_k[C_A]_k - \gamma[K] \end{bmatrix} \begin{Bmatrix} \{c_R\}_k \\ \{c_I\}_k \end{Bmatrix} = \begin{Bmatrix} \{0\} \\ \{P\}_k \end{Bmatrix}; \quad k = 1,\ldots,K_d \tag{18}$$

where $\gamma$ is the structural damping factor. The displacements $\{u\}_k$ are subsequently obtained from

$$\{u\}_k = \{c_R\}_k \sin \Omega_k^t + \{c_I\}_k \cos \Omega_k t \tag{19}$$

For the $j$th degree of freedom the dynamic displacement may be written in terms of its magnitude and phase angle as

$$u_{jk} = |u_{jk}| \sin (\Omega_k t + \phi_{jk}) \tag{20}$$

where

$$|u_{jk}| = (c_{R_{jk}}^2 + c_{I_{jk}}^2)^{1/2} \tag{21}$$

and

$$\tan \phi_{jk} = c_{I_{jk}}/c_{R_{jk}} \tag{22}$$

The dynamic actuator forces are subsequently obtained by substituting the dynamic displacements and their time derivatives into Eq. (16).[19]

**Approximate Problem Generation**

Each approximate problem is constructed through the use of a variety of techniques known as approximation concepts.[20–22] The approximation concepts used here include: 1) design variable linking, 2) temporary constraint deletion, and 3) explicit objective and constraint function approximations.

Design variable linking is used to reduce the number of independent design variables in the problem. Here, the design variables associated with a structural member can be linked to those of selected other members, resulting in all of these members being the same size. Likewise, the design variables associated with selected control elements can be linked together so that the feedback gains for a selected group of actuators are identical.

To reduce the number of constraints in the design problem and the associated computational burden, it is possible to temporarily delete certain constraints that are not expected to currently participate in the design process. A relatively simple, but effective, strategy for constraint deletion consists of temporarily ignoring all constraints with response ratios less than some specified constraint truncation parameter (CTP). Here, the value of CTP is either set to a user prescribed value or it is calculated automatically such that: 1) all constraints with $R_q \geq 0.7$ are retained, 2) all constraints with $R_q < 0.3$ are deleted, and 3) constraints with $0.3 \leq R_q < 0.7$ are retained or deleted depending on the value of the response ratio cutoff value $R_c$. This criterion can be written as

$$\text{CTP} = \min\,[\max\{R_c,\ 0.3\},\ 0.7] \tag{23}$$

where $R_c$ is the maximum response ratio rounded down to the nearest tenth. When CTP is prescribed by the user, it is held constant during the entire design process. Otherwise, the value of CTP is updated for each approximate problem.

The key to the efficient solution of the synthesis problems posed here lies in the construction of useful explicit objective function and constraint approximations. While higher-order approximations are possible, first-order approximations are most attractive, since only the first derivatives of the functions which are to be approximated are required. A particularly useful approximation, first proposed in Ref. 25, is based on the selective expansion of the function into terms depending either on the direct design variable or its reciprocal. This leads to a nonlinear approximation that is conservative with respect to both pure linear and pure inverse approximations. This approximation has the following form (shown here for the constraint function $g_q$):

$$\tilde{g}_q(Y) \simeq g_q(Y_0) + \sum_{b=1}^{B} \frac{\partial g_q(Y_0)}{\partial Y_b} C_{bq} \leq 0 \tag{24}$$

where

$$C_{bq} = Y_b - Y_{0_b} \quad \text{if} \quad \frac{\partial g_q(Y_0)}{\partial Y_b} > 0$$
$$= -Y_{0_b}^2\left(\frac{1}{Y_b} - \frac{1}{Y_{0_b}}\right) \quad \text{if} \quad \frac{\partial g_q(Y_0)}{\partial Y_b} < 0 \tag{25}$$

The derivatives of the objective function and constraints with respect to the design variables are obtained from chain rule operations and, for the general case, require the calculation of the derivatives of the system response quantities with respect to the structural and control element properties. Methods for calculating the static displacement and natural frequency sensitivities are well known.[26] The derivatives of the magnitudes of the dynamic displacements are obtained by implicitly differentiating Eq. (21). The derivatives of the magnitudes of the actuator forces are obtained similarly.[19] In both cases, the requisite derivatives of $\{c_R\}_k$ and $\{c_I\}_k$ are obtained by differentiating Eq. (18) with respect to the element properties (see the Appendix). These derivatives are conveniently calculated in the same way that the static displacement sensitivities are calculated. Here, the partial inverse form of the pseudoload method[21,27] is used.

While the objective function and constraint approximations described above are constructed to be of high quality, these approximations do not, in general, accurately represent the true functions over the entire design space. To ensure that the approximations remain valid during the solution of each approximate problem, stepwise move limits are employed to temporarily restrict the design space to a region over which the approximating functions are believed to be valid. The stepwise upper and lower bounds are calculated from a designer-supplier move limit parameter $d_m$ as

$$\tilde{Y}_b^L = \max\,[Y_b^L,\ Y_b - d_m Y_b] \tag{26}$$

$$\tilde{Y}_b^U = \min\,[Y_b^U,\ Y_b + d_m Y_b] \tag{27}$$

where $Y_b$ is the value of the $b$th design variable at the beginning of each approximate problem step and $Y_b^U$ and $Y_b^L$ the original side constraints on $Y_b$ [see Eq. (1)].

#### Optimization

Each of the approximate problems constructed as described in the previous section is an explicit, separable, convex inequality constrained mathematical programming problem. As such, each of these problems can be solved using any one of a number of well-known nonlinear constrained minimization techniques. The method chosen here is a feasible directions method as implemented in the CONMIN[28] optimization program. In addition, for approximate problems associated with the response and control force minimization problems [Eqs. (4) and (5)], an explicit dual function can be constructed.[29] These explicit dual functions can be maximized (subject to non-negativity constraints on the dual variables) using various algorithms; in this work, CONMIN is used for convenience. The dual formation is usually more efficient when the number of retained constraints is less than the number of design variables.

## Numerical Results

The control-augmented structural synthesis methodology described in this paper has been implemented in a research computer program. The program has been used to generate numerical results for numerous example problems,[19] several of which are described here. These problems were selected so that, in addition to demonstrating the basic features of the design methodology, the results could be critically evaluated through insights into the physical behavior of the system.

#### Problem 1—Cantilevered Beam, Mass Minimization

The first example problem is that of finding the minimum mass design of a cantilevered beam shown in Fig. 3. The beam is modeled with 10 beam-type finite elements, each 1.0 m in length. The motion of the beam is constrained such that only vertical displacements and in-plane rotations are allowed. A concentrated mass (200 kg) is located at the midspan node and a vertical harmonic loading [$P_1(t) = 4000$ N sin (3.9 Hz)$t$] is applied at the tip. Structural damping ($\gamma = 0.02$) of 2% is assumed.

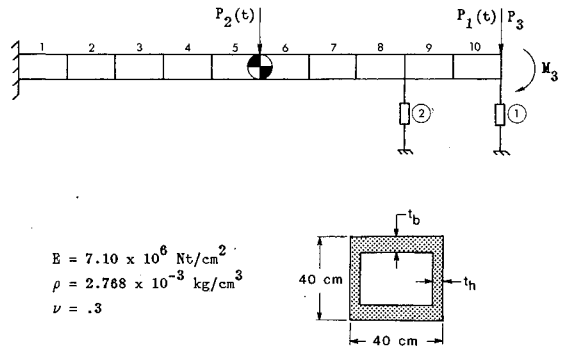


Fig. 3 Cantilevered beam, problems 1–4.

**Table 1 Iteration history data for problem 1: cantilevered beam, mass minimization**

| Analysis | Mass, kg [maximum constraint violation, %] Uncontrolled | Controlled 1 actuator | Controlled 2 actuators |
|---|---|---|---|
| 0 | 1937.60 [241.4] | 1937.60 [244.1] | 1937.60 [96.8] |
| 1 | 1435.58 [5.0] | 1445.70 [2.0] | 1451.64 [0.0] |
| 2 | 1060.17 [0.0] | 1055.86 [0.0] | 1051.61 [0.0] |
| 3 | 774.72 [0.0] | 768.06 [0.0] | 762.12 [0.0] |
| 4 | 571.01 [0.0] | 563.48 [0.0] | 557.37 [0.0] |
| 5 | 428.23 [0.0] | 420.22 [0.0] | 413.16 [0.0] |
| 6 | 329.83 [0.0] | 318.91 [0.0] | 311.01 [0.0] |
| 7 | 293.13 [0.0] | 279.29 [0.0] | 270.72 [0.0] |
| 8 | 292.16 [0.0] | 276.10 [1.6] | 267.58 [1.0] |
| 9 | 292.16 [0.0] | 275.51 [0.0] | 266.83 [0.0] |
| 10 | | 274.68 [0.0] | 266.09 [0.0] |

**Table 2 Final designs for problem 1: cantilevered beam, mass minimization**

| Element type | Element No. 1 | Design variables | Final design Uncontrolled | Controlled 1 actuator | Controlled 2 actuators |
|---|---|---|---|---|---|
| Frame | 1-2 | $t_b$, cm | 1.6100 | 1.3974 | 1.2824 |
| | 3-4 | $t_b$, cm | 1.0570 | 0.8998 | 0.8156 |
| | 5-6 | $t_b$, cm | 0.5350 | 0.5000$^-$ | 0.5000$^-$ |
| | 7-8 | $t_b$, cm | 0.5000$^{-a}$ | 0.5000$^-$ | 0.5000$^-$ |
| | 9-10 | $t_b$, cm | 0.5000$^-$ | 0.5000$^-$ | 0.5000$^-$ |
| | 1-10 | $t_h$, cm | 0.5000$^-$ | 0.5000$^-$ | 0.5000$^-$ |
| Control | 1 | $h_p$, N/cm | | 74.3907 | 75.2934 |
| | | $h_v$, N · s/cm | | 1.2213 | 1.0236 |
| | 2 | $h_p$, N/cm | | | 79.4161 |
| | | $h_v$, N · s/cm | | | 1.5079 |

[a] – denotes lower-bound value.

The design variables for this problem are the web and flange thicknesses $(t_h,t_b)$ of the beam elements and the position and velocity feedback gains $(h_p,h_v)$ of the control elements. The beam element thicknesses are linked pairwise along the length of the structure, resulting in 10 independent structural design variables. The initial values of these variables was taken to be 5.0 cm with side constraints imposed so that $0.5 \leq t_b,\ t_h \leq 10.0$ cm.

Three runs were made for this problem. In each run, the magnitude of the vertical dynamic tip displacement is constrained to be less than 10.0 cm and the first open-loop frequency must be greater than 4.0 Hz. Stepwise move limits of 30% ($d_m = 0.3$) were imposed on the design variables. In the first run (uncontrolled), there are no active control devices in the system. For the second run, actuator 1 is added to the system and both actuators 1 and 2 are included in the final run. The initial values of the feedback gains are $h_p = 20.0$ N/cm and $h_v = 5.0$ N · s/cm. Lower-bound side constraints on the feedback gains ($h_p \geq 0.05$ N/cm, $h_v = 0.05$ N · s/cm) ensure that the final designs will be dynamically stable.[15] The magnitudes of the actuator forces are constrained to be less than 20% of the external loading (800 N) and the total control force must be less than 35% of the loading (1400 N).

The iteration history data and final designs for all three runs are given in Tables 1 and 2. In all three runs, the tip displacement constraint is critical for the final design. The outboard actuator force constraint is also critical in both the controlled runs and the total control force constraint is critical in the final run. It is interesting to note that, when two actuators are included in the system, the outboard actuator is favored in the final design. This is not unexpected since, for these problems, the open-loop frequencies are all greater than the forcing function frequency and, as a result, the dynamic response is dominated by first-mode behavior.

For all three runs, the structural designs are changed from an initial uniform thickness distribution to the intuitively satisfying final designs in which the web thickness $t_h$ takes on its minimum gage value. Also, the flange thicknesses $t_b$ are tapered along the length of the beam from a maximum value at the root to minimum gage at the tip. This tapered design is to be expected when the dynamic response is dominated by first-mode behavior.

It is also interesting to observe that the actuator position gains $h_p$ consistently dominate the velocity gains $h_v$ for the final designs. This is primarily due to the fact that the open-loop frequencies are well above the forcing function frequency, resulting in the stiffness augmentation being relatively more effective (as compared to damping augmentation) in reducing the steady-state response.

Examination of the objective function values for the final designs shows a large improvement over the initial infeasible designs for all runs. Also, small (6–9%) improvements in the final design mass are obtained as the actuators are added to the system.

### Problem 2—Cantilevered Beam, Response Minimization

In the second example, the design goal is to minimize the dynamic tip displacement of the cantilevered beam shown in Fig. 3. The loading, design variables, initial design, behavior constraints, and side constraints are the same as those for problem 1. In addition, an upper-bound constraint of 1000 kg is imposed on the structural mass.

Again, three runs were made for this problem with the stepwise move limits of 40% imposed on the design variables. In this case, each approximate problem is solved in its dual form. The iteration history data and final designs are given in Tables 3 and 4. The structural mass constraint is critical for all final

designs and the outboard actuator force constraint is critical for both controlled runs. For the final run, the total control force constraint is also critical, with the outboard actuator being favored over the inboard actuator due to its high effectiveness in controlling the tip response.

It is interesting to observe that the final structural designs are virtually identical for all three runs. This is intuitively satisfying since it is expected that the limited amount of structural material will exhibit a unique optimal distribution. As in problem 1, the contributions to the actuator forces due to velocity feedback are small compared to that due to position feedback. Again, this is due to the relative ineffectiveness of damping augmentation away from a resonance condition.

Finally, examination of the final design objective function values shows a large improvement over the initial infeasible designs for all runs. Also, significant improvements (20–30%) in the final design objective function values are realized with the addition of active control.

**Problem 3—Cantilevered Beam, Control Force Minimization**

In this example, the design goal is to minimize the total control force for the control augmented cantilevered beam shown in Fig. 3. The loading, design variables, side constraints, and frequency constraint are the same as in problem 1. In this case, the magnitude of the tip displacement is constrained to be less than 4.0 cm. The magnitudes of the actuator forces must be less than 4000 N and the structural mass must be less than 400 kg.

Three runs were made for this problem. In the first run, only actuator 1 is included in the system model. Only actuator 2 is included for the second run, while in the final run both actuators are included. In this problem, stepwise move limits of 40% are used. The initial designs for runs 1 and 3 are given by $t_b = 2.0$ cm, $t_h = 0.75$ cm, $h_p = 50.0$ N/cm, and $h_v = 5.0$ N · s/cm.

For the second run, the initial design was $t_b = 2.0$ cm, $t_h = 0.75$ cm, $h_p = 100.0$ N/cm, and $h_v = 7.5$ N · s/cm. The iteration history data and final designs are given in Tables 5 and 6. The structural mass and tip displacement constraints are critical for all three final designs.

Comparison of the final design objective function values underscores the importance of proper selection of the actuator location. Clearly, when the actuator is placed at the inboard position, rather than at the tip, the required control force is significantly greater (49.9%). This is due to the fact that the first structural mode is more readily controlled at the outboard position. In the final run, where both actuators are included, the inboard actuator tends to "vanish" in favor of the outboard actuator. Although the objective function valued attained is slightly greater (6.9%) than that of run 1, a difference of less than 1.7% was obtained in a subsequent run where a tighter convergence criterion was used.

Finally, it should be noted that the final structural designs for all three runs are nearly identical. Again, as in problem 2, this is an indication of an essentially unique optimal material distribution (given a limited amount of material) for the problem.

**Problem 4—Cantilevered Beam, Multiple Loading Conditions**

This problem is the same as problem 1, except that three independent loading conditions are considered. The three loading conditions are given by $P_1(t) = 4000$ N $\sin(3.9\text{ Hz})t$, $P_2(t) = 4000$ N $\sin(5.0\text{ Hz})t$, and $P_3 = 4000$ N, $M_3 = 2.0 \times 10^5$ N · cm, respectively. Note that the third loading condition

**Table 3 Iteration history data for problem 2: cantilevered beam, response minimization**

| | Tip displacement, cm [maximum constraint violation, %] | | |
|---|---|---|---|
| Analysis | Uncontrolled | Controlled 1 actuator | Controlled 2 actuators |
| 0 | 24.14 [241.4] | 15.73 [244.1] | 12.86 [99.6] |
| 1 | 15.51 [55.1] | 10.84 [40.9] | 7.46 [26.2] |
| 2 | 20.87 [208.7] | 11.43 [27.1] | 3.23 [0.0] |
| 3 | 4.20 [0.0] | 4.60 [0.0] | 2.05 [0.2] |
| 4 | 2.71 [0.0] | 2.81 [0.0] | 1.65 [0.0] |
| 5 | 2.12 [0.0] | 2.03 [0.0] | 1.48 [0.0] |
| 6 | 1.93 [0.3] | 1.72 [0.7] | 1.36 [3.1] |
| 7 | 1.85 [0.2] | 1.55 [0.2] | 1.27 [6.6] |
| 8 | 1.81 [0.2] | 1.45 [0.3] | 1.27 [0.8] |
| 9 | 1.79 [0.0] | 1.43 [0.7] | 1.26 [0.6] |
| 10 | 1.79 [0.0] | 1.43 [0.7] | 1.26 [0.9] |
| 11 | 1.79 [0.0] | 1.43 [0.2] | 1.25 [0.2] |

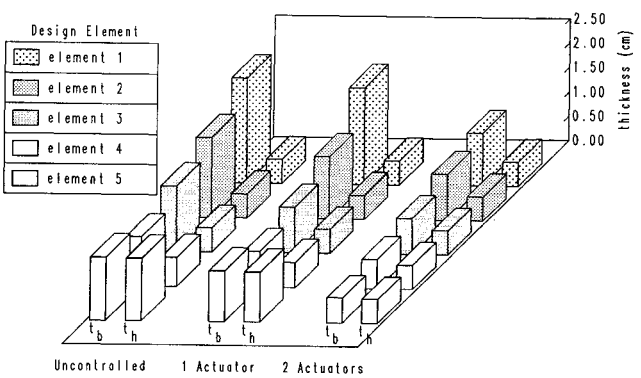


**Fig. 4 Final design thickness distribution, problem 4.**

**Table 4 Final designs for problem 2: cantilevered beam, response minimization**

| | | | Final design | | |
|---|---|---|---|---|---|
| Element type | Element nos. | Design variables | Uncontrolled | Controlled 1 actuator | Controlled 2 actuators |
| Frame | 1-2 | $t_b$, cm | 8.2810 | 8.2805 | 8.2701 |
| | 3-4 | $t_b$, cm | 6.2360 | 6.2388 | 6.2426 |
| | 5-6 | $t_b$, cm | 3.8119 | 3.8149 | 3.8490 |
| | 7-8 | $t_b$, cm | 1.7654 | 1.7634 | 1.7670 |
| | 9-10 | $t_b$, cm | 0.5000[a] | 0.5000[a] | 0.5000[a] |
| | 1-10 | $t_h$, cm | 0.5000[a] | 0.5000[a] | 0.5000[a] |
| Control | 1 | $h_p$, N/cm | | 554.9204 | 635.5459 |
| | 2 | $h_v$, N · s/cm | | 3.3034 | 3.0415 |
| | | $h_p$, N/cm | | | 739.5169 |
| | | $h_v$, N · s/cm | | | 4.1872 |

[a] – denotes lower-bound value.

is static loading condition (see Fig. 3). In addition to the constraints imposed in problem 1, the static tip rotation is constrained to be less than 0.00796 rad and the lowest open-loop frequency must lie between 4.0 and 4.9 Hz. The upper bound on the total control force (summed over the two dynamic load conditions) is 2800 N.

Three runs were made for this problem using stepwise move limits of 30%. The iteration history data and final designs are given in Tables 7 and 8. The dynamic tip displacement constraints (under both loading conditions) and the upper-bound frequency constraints are either critical or near critical for all three final designs. In addition, the outboard actuator force constraint (under load condition 1) is critical in the second run and, in the final run, the static rotation constraint and both actuator force constraints (under load condition 1) are critical.

For this problem, several interesting observations can be made from the final design data. First, for the uncontrolled run, the final structural material distribution exhibits characteristics typical of a mass damper type of solution. Specifically, while the flange thickness distribution initially tapers from the

**Table 5 Iteration history data for problem 3: cantilevered beam, control force minimization**

| | Control force, N [maximum constraint violation, %] | | |
|---|---|---|---|
| Analysis | Actuator 1 | Actuator 2 | Combined |
| 0 | 1191.2 [225.0] | 1378.0 [228.1] | 1847.8 [202.7] |
| 1 | 1269.4 [42.4] | 1434.3 [47.1] | 1841.1 [33.6] |
| 2 | 1617.8 [8.2] | 1805.5 [14.2] | 1625.6 [5.4] |
| 3 | 1343.8 [0.0] | 1543.5 [0.0] | 1318.3 [0.0] |
| 4 | 1127.9 [0.0] | 1409.1 [0.0] | 1167.0 [0.0] |
| 5 | 964.6 [0.0] | 1341.9 [0.0] | 1074.7 [0.0] |
| 6 | 902.2 [0.0] | 1251.4 [0.0] | 997.4 [0.0] |
| 7 | 842.9 [0.0] | 1231.9 [0.0] | 950.9 [0.0] |
| 8 | 822.0 [0.1] | 1218.4 [0.1] | 897.1 [0.0] |
| 9 | 812.2 [0.1] | 1214.8 [0.1] | 879.2 [0.1] |
| 10 | 811.4 [0.1] | 1214.8 [0.1] | 871.1 [0.0] |
| 11 | 810.5 [0.1] | | 867.4 [0.1] |
| 12 | | | 866.6 [0.1] |

**Table 6 Final designs for problem 3: cantilevered beam, control force minimization**

| Element type | Element nos. | Design variables | Final design | | |
|---|---|---|---|---|---|
| | | | Actuator 1 | Actuator 2 | Combined |
| Frame | 1-2 | $t_b$, cm | 2.7099 | 2.7013 | 2.6999 |
| | 3-4 | $t_b$, cm | 1.9018 | 1.8976 | 1.9151 |
| | 5-6 | $t_b$, cm | 1.0813 | 1.1018 | 1.0857 |
| | 7-8 | $t_b$, cm | 0.5000[a] | 0.5000[-] | 0.5000[-] |
| | 9-10 | $t_b$, cm | 0.5000[-] | 0.5000[-] | 0.5000[-] |
| | 1-10 | $t_h$, cm | 0.5000[-] | 0.5000[-] | 0.5000[-] |
| Control | 1 | $h_p$, N/cm | 196.9884 | | 172.6867 |
| | 2 | $h_v$, N · s/cm | 1.9062 | | 1.5341 |
| | | $h_p$, N/cm | | 452.6438 | 52.3790 |
| | | $h_v$, N · s/cm | | 4.1980 | 1.2029 |

[a] – denotes lower-bound value.

**Table 7 Iteration history data for problem 4: cantilevered beam, multiple loading conditions**

| | Mass, kg [maximum constraint violation, %] | | |
|---|---|---|---|
| Analysis | Uncontrolled | Controlled 1 actuator | Controlled 2 actuators |
| 0 | 1937.60 [241.4] | 1937.60 [244.1] | 1937.60 [199.6] |
| 1 | 1435.58 [5.0] | 1445.70 [2.0] | 1450.12 [0.0] |
| 2 | 1060.25 [0.0] | 1056.75 [0.0] | 1050.51 [0.0] |
| 3 | 774.67 [0.0] | 764.82 [0.0] | 762.41 [0.0] |
| 4 | 586.29 [0.0] | 559.22 [0.0] | 559.19 [0.0] |
| 5 | 525.75 [0.0] | 482.77 [1.2] | 434.07 [0.0] |
| 6 | 502.78 [0.0] | 446.32 [0.0] | 363.08 [0.0] |
| 7 | 491.28 [0.0] | 425.22 [0.7] | 318.91 [0.3] |
| 8 | 484.39 [0.0] | 409.00 [0.0] | 297.34 [0.0] |
| 9 | 478.81 [0.0] | 399.44 [0.3] | 288.51 [0.0] |
| 10 | 476.29 [0.0] | 397.69 [0.1] | 288.40 [0.3] |
| 11 | 475.00 [0.0] | 397.20 [0.0] | 283.72 [0.0] |
| 12 | 473.58 [0.0] | 397.03 [0.0] | 281.41 [0.0] |
| 13 | 473.18 [0.1] | 396.90 [0.0] | 281.20 [0.0] |
| 14 | 473.18 [0.1] | | 281.20 [0.0] |

**Table 8 Final Design for problem 4: cantilevered beam, multiple loading conditions**

| Element type | Element nos. | Design variables | Final design: Uncontrolled | Final design: Controlled 1 actuator | Final design: Controlled 2 actuators |
|---|---|---|---|---|---|
| Frame | 1-2 | $t_b$, cm | 2.1628 | 1.9997 | 1.0930 |
| | 3-4 | $t_b$, cm | 1.6528 | 1.2940 | 0.9583 |
| | 5-6 | $t_b$, cm | 1.3692 | 0.9611 | 0.7579 |
| | 1-6 | $t_n$, cm | 0.5000[a] | 0.5000[a] | 0.5000[a] |
| | 7-8 | $t_b$, cm | 1.0222 | 0.7462 | 0.6138 |
| | | $t_h$, cm | 0.6024 | 0.5308 | 0.5000[a] |
| | 9-10 | $t_b$, cm | 1.3199 | 1.0629 | 0.5251 |
| | | $t_n$, cm | 1.3012 | 1.0493 | 0.5000[a] |
| Control | 1 | $h_p$, N/cm | | 20.7929 | 68.3930 |
| | | $h_v$, N · s/cm | | 3.1488 | 1.6856 |
| | 2 | $h_p$, N/cm | | | 96.0628 |
| | | $h_v$, N · s/cm | | | 2.4295 |

[a] — denotes lower-bound value.

root toward the tip, it increases again for the outboard elements (see Fig. 4). Also, the web thickness is significantly greater than its lower-bound value near the tip. Both of these conditions combine to simulate a nonstructural mass near the tip of the beam. This behavior is also seen, to a lesser degree, in the final design for run 2. The existence of mass damper charactreistics in these designs results from the upper bound on the open-loop frequency that prohibits the purely tapered designs achieved in problem 1.

It is also interesting to note that the contribution to the actuator forces due to the velocity feedback is more significant for this problem than it was in problems 1–3. This is due to the fact that the first natural frequencies for the final structual designs are near the 5.0 Hz forcing function frequency. As a result, the effectiveness of the damping augmentation in controlling the steady-state response is increased.

The addition of the inboard actuator in the third run resulted in satisfaction of the dynamic displacement constraints without resorting to a mass damper type of design. In this case, the structural stiffness was allowed to decrease enough to cause the static tip rotation constraint to become critical.

Finally, examination of the final design objective function values shows a significant decrease (16–49%) in the structural mass with the introduction of active control.

**Problem 5—Grillage**

The final example problem involves the design of the 8 × 11 planar grillage shown in Fig. 5. The grillage, similar to the one described in Ref. 30, consists of a lattice of 19 aluminum frame members ($\rho = 0.1$ lb/in$^3$, $E = 10.5 \times 10^6$ psi, $\nu = 0.3$) placed on 1 ft centers and cantilevered from two fixed supports by 20 in. long flexible beams. Each member is 2.0 in. wide and has an initial thickness of 0.25 in. The members are oriented so that the width dimension lies in the plane of the structure. The grillage is augmented with 24 active control elements uniformly distributed over the grillage acting in the $z$ direction. The mass of each actuator ($1.296 \times 10^{-3}$ lb · s$^2$/in.) is modeled as fixed nonstructural mass. The grillage is subjected to a dynamic loading [$P(t) = 16.9$ lb sin (2.0 Hz)$t$] applied at node 6 in the $z$ direction. Structural damping of 2% is assumed.

Two runs were made for this problem. In the first run (control force minimization), the design goal is to minimize the total control force subject to upper-bound constraints of 1.0 in. on the magnitudes of the out-of-plane dynamic displacements at the four corners of the grillage. The design variables are the control element position and velocity feedback gains and they are initially set to $h_p = 0.1$ lb/in. and $h_v = 0.025$ lb · s/in. for all actuators. Lower bounds are imposed on the gains so that $h_p \geq 0.001$ lb/in. and $h_v \geq 0.001$ lb · s in. The design variables associated with each actuator are linked with those of the actuator located at its symmetric grid point (see $y$-$z$ plane Fig. 5) resulting in 24 independent design variables. Actuator force

**Table 9 Iteration history data for problem 5: grillage**

| Analysis | Objective function, lb [maximum constraint violation, %]: Control force | Weight |
|---|---|---|
| 0 | 9.00 [2.2] | 94.20 [249.4] |
| 1 | 18.53 [0.0] | 89.82 [0.0] |
| 2 | 11.73 [0.0] | 85.43 [0.0] |
| 3 | 7.29 [0.0] | 77.42 [6.1] |
| 4 | 6.70 [0.0] | 67.94 [0.0] |
| 5 | 5.94 [0.0] | 61.76 [0.0] |
| 6 | 5.32 [0.0] | 59.00 [0.0] |
| 7 | 4.66 [0.0] | 58.02 [0.2] |
| 8 | 4.50 [0.0] | 58.04 [0.0] |
| 9 | 3.68 [0.0] | 57.55 [0.0] |
| 10 | 3.65 [0.0] | 57.07 [0.4] |
| 11 | 3.61 [0.0] | 56.85 [0.0] |
| 12 | | 56.72 [0.0] |
| 13 | | 56.14 [0.4] |
| 14 | | 55.57 [0.1] |
| 15 | | 55.49 [0.0] |

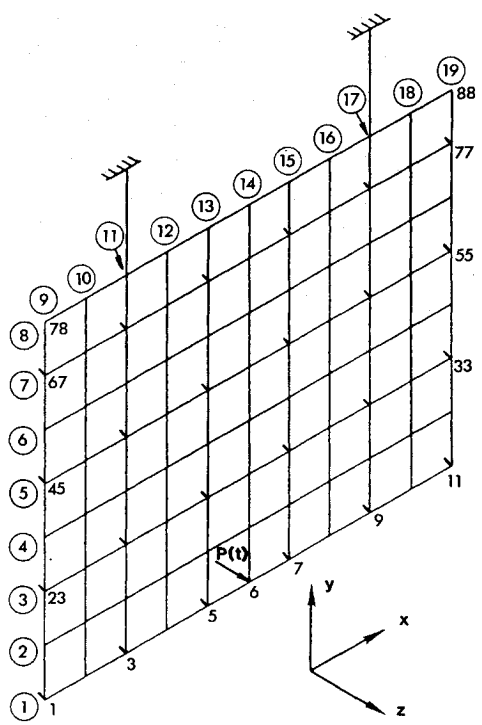


Fig. 5 Grillage, problem 5.

**Table 10 Actuator Forces for problem 5: grillage**

| Actuator location (grid no.) | Actuator forces, lb | | |
|---|---|---|---|
| | Initial | Control force minimization | Weight minimization |
| 1,11 | 0.6396 | 0.0277 | 0.1339 |
| 3,9 | 1.0144 | 0.1116 | 0.0872 |
| 5,7 | 1.0571 | 0.4320 | 0.0397 |
| 23,33 | 0.3260 | 0.0321 | 0.1297 |
| 25,31 | 0.5777 | 0.0242 | 0.0618 |
| 27,28 | 0.5754 | 0.0207 | 0.0730 |
| 45,55 | 0.9735 | 0.4037 | 0.3301 |
| 47,53 | 1.0011 | 0.0635 | 0.0900 |
| 49,51 | 0.8194 | 0.0455 | 0.0754 |
| 67,77 | 0.9138 | 0.5201 | 0.5506 |
| 69,75 | 0.7511 | 0.0712 | 0.0877 |
| 71,73 | 0.6155 | 0.0529 | 0.0759 |

constraints are also employed to limit each actuator output to a maximum of 2.0 lb. Note that the structural design is fixed ($w = 2.0$ in., $t = 0.25$ in.) for this run.

In the second run (weight minimization), the design goal is to minimize the structural weight of the grillage. In this case, both the actuator gains and the structural member thickness are included as design variables. The initial values and lower bounds for the gains are the same as in run 1. The member thicknesses are initially 0.25 in., with side constraints imposed so that $0.1 \leq t \leq 0.5$ in. In addition to the dynamic displacement and actuator force constraints, an upper-bound constraint is imposed on the total control force for this run. The upper-bound value was chosen to be equal to the final design value of the total control force for run 1 (3.61 lb).

Iteration history data as well as initial and final design actuator forces for these runs are given in Tables 9 and 10. A significant reduction (60%) in the total control force was realized in run 1 by redistributing the actuator forces to more efficiently control the second and third structural modes.

For the second run, the final structural design is such that all of the members achieve the lower bound thickness value (0.1 in.) except for members 2, 8, 11, and 17. The final thickness values for these members are $t_2 = 0.2993$ in., $t_8 = 0.2284$ in., and $t_{11} = t_{17} = 0.3959$ in. It should be noted that, although symmetry of the actuator gains was enforced through design variable linking, the expected structural symmetry in the final design was obtained without linking. Also, the thicknesses of the main load-carrying members of the grillage (11 and 17) has increased by 58%. Finally, a 58.9% reduction in the structural weight was obtained with no increase in the total control force over that of run 1.

## Summary

A synthesis methodology for the design of a structure and its associated active control system has been set forth in which independent sets of design variables associated with the structure and the control system are treated simultaneously. While inherently more general, the method has been demonstrated for structures subjected to static and harmonic dynamic loading conditions for which the steady-state response is of primary interest. The direct treatment of an extensive mix of constraints (i.e., static and dynamic displacement constraints, actuator force level constraints, and open-loop frequency constraints) is featured in this work.

The numerical examples presented here serve to underscore the importance of integrating the structural and control system design process. While the extent to which the structural and/or control system design can be improved is apparently problem dependent, it is clear that the best designs are obtained when the structure and control system are designed simultaneously. It has again been demonstrated that significant reductions in control force can be realized through structural modifications. In addition, it was observed that the addition of an active control system to a structure can lead to significant reductions in response and/or structural mass.

## Appendix

The derivatives of the steady-state dynamic displacements with respect to the structural element section properties and control element feedback gains can be obtained through the implicit differentiation of Eq. (19) with respect to the $j$th property of the $i$th element, giving

$$\frac{\partial\{u\}_k}{\partial x_{ij}} = \frac{\partial\{c_R\}_k}{\partial x_{ij}} \sin \Omega_k t + \frac{\partial\{c_I\}_k}{\partial x_{ij}} \cos \Omega_k t \tag{A1}$$

where it is assumed that $\Omega_k$ is independent of $x_{ij}$. Similarly, the derivatives of the magnitude of the $r$th dynamic displacement are obtained by differentiating Eq. (21) with respect to $x_{ij}$, yielding

$$\frac{\partial|u_{rk}|}{\partial x_{ij}} = \frac{1}{|u_{rk}|}\left[c_{R_{rk}} \frac{\partial c_{R_{rk}}}{\partial x_{ij}} + c_{I_{rk}} \frac{\partial c_{I_{rk}}}{\partial x_{ij}}\right] \tag{A2}$$

In both cases, the derivatives of $\{c_R\}$ and $\{c_I\}$ with respect to $x_{ij}$ are required. These derivatives are given by the implicit differentiation of Eq. (18). Writing Eq. (18) in the following compact notation:

$$\begin{bmatrix} [A]_k & [B]_k \\ [B]_k & -[A]_k \end{bmatrix} \begin{Bmatrix} \{c_R\}_k \\ \{c_I\}_k \end{Bmatrix} = \begin{Bmatrix} \{0\} \\ \{P\}_k \end{Bmatrix} \tag{A3}$$

and differentiating with respect to $x_{ij}$ gives

$$\begin{bmatrix} \dfrac{\partial[A]_k}{\partial x_{ij}} & \dfrac{\partial[B]_k}{\partial x_{ij}} \\ \dfrac{\partial[B]_k}{\partial x_{ij}} & \dfrac{-\partial[A]_k}{\partial x_{ij}} \end{bmatrix} \begin{Bmatrix} \{c_R\}_k \\ \{c_I\}_k \end{Bmatrix} + \begin{bmatrix} [A]_k & [B]_k \\ [B]_k & -[A]_k \end{bmatrix} \begin{Bmatrix} \dfrac{\partial\{c_R\}_k}{\partial x_{ij}} \\ \dfrac{\partial\{c_I\}_k}{\partial x_{ij}} \end{Bmatrix}$$

$$= \begin{Bmatrix} \{0\} \\ \dfrac{\partial\{P\}_k}{\partial x_{ij}} \end{Bmatrix} \tag{A4}$$

Under the assumption that $\{P\}_k$ is independent of $x_{ij}$, Eq. (A4) can be written as

$$\begin{bmatrix} [A]_k & [B]_k \\ [B]_k & -[A]_k \end{bmatrix} \begin{Bmatrix} \dfrac{\partial\{c_R\}_k}{\partial x_{ij}} \\ \dfrac{\partial\{c_I\}_k}{\partial x_{ij}} \end{Bmatrix} = \begin{Bmatrix} V_{I_{ijk}} \\ V_{R_{ijk}} \end{Bmatrix} \tag{A5}$$

where the pseudoload vectors $V_{I_{ijk}}$ and $V_{R_{ijk}}$ are given by

$$V_{I_{ijk}} = -\frac{\partial[A]_k}{\partial x_{ij}} \{c_R\}_k - \frac{\partial[B]_k}{\partial x_{ij}} \{c_I\}_k \tag{A6}$$

and

$$V_{R_{ijk}} = -\frac{\partial[B]_k}{\partial x_{ij}} \{c_R\}_k + \frac{\partial[A]_k}{\partial x_{ij}} \{c_I\}_k \tag{A7}$$

Substituting for $[A]_k$ and $[B]_k$ [see Eq. (18)], Eqs. (A6) and (A7) become

$$V_{I_{ijk}} = -\left[\Omega_k \frac{\partial[C_A]_k}{\partial x_{ij}} + \gamma \frac{\partial[K]}{\partial x_{ij}}\right]\{c_R\}_k - \left[\frac{\partial[K_A]_k}{\partial x_{ij}} - \Omega_k^2 \frac{\partial[M]}{\partial x_{ij}}\right]\{c_I\}_k \tag{A8}$$

$$V_{R_{ijk}} = -\left[\frac{\partial[K]_k}{\partial x_{ij}} - \Omega_k^2 \frac{\partial[M]}{\partial x_{ij}}\right]\{c_R\}_k + \left[\Omega_k \frac{\partial[C_A]_k}{\partial x_{ij}} + \gamma \frac{\partial[K]}{\partial x_{ij}}\right]\{c_I\}_k \tag{A9}$$

The derivatives of $\{c_R\}_k$ and $\{c_I\}_k$ can be obtained directly by back substitution of the pseudoload vectors into the previously decomposed dynamic response matrix. It should be recognized that this is analogous to the pseudoload method for calculating static displacement derivatives and that computational efficiency can be maintained through the implementation of the method in its partial inverse form.

## Acknowledgment

This research was supported by NASA Research Grant NSG 1490.

## References

[1]Nurre, G. S., Ryan, R. S., Scofield, H. N., and Sims, J. L., "Dynamics and Control of Large Space Structures," *Journal of Guidance, Control and Dynamics*, Vol. 7, Sept-Oct. 1984, pp. 514–526.

[2]Trudell, R. W., Curley, R. C., and Rogers, L. C., "Passive Damping in Large Precision Space Structures," *Proceedings of the 21st AIAA/ASME/ASCE/AHS Structures, Structural Dynamics and Materials Conference*, AIAA, Washington, DC, May 1980, pp. 124–136.

[3]Garibotti, J. F., "Requirements and Issues for the Control of Flexible Space Structures," *Proceedings of the 25th AIAA/ASME/ASCE/AHS Structures, Structural Dynamics and Materials Conference*, AIAA, Washington, DC, 1984, pp. 338–347.

[4]Venkayya, V. B. and Tischler, V. A., "Frequency Control and the Effect on Dynamic Response of Flexible Structures," *Proceedings of the 25th AIAA/ASME/ASCE/AHS Structures, Structural Dynamics and Materials Conference*, AIAA, Washington, DC, May, 1984, pp. 431–441.

[5]Haftka, R. T., Martinovic, Z. N., and Hallauer, W. L., "Enhanced Vibration Controllability by Minor Structural Modifications," *AIAA Journal*, Vol. 23, 1985, pp. 1260–1266.

[6]Haftka, R. T., Martinovic, Z. N., Hallauer, W. L., and Schamel, G., "Sensitivity of Optimized Control Systems to Minor Structural Modifications," *Proceedings of the 26th AIAA/ASME/ASCE/AHS Structures, Structural Dynamics and Materials Conference*, AIAA, Washington, DC, April, 1985, pp. 642–650.

[7]Messac, A. and Turner, J., "Dual Structural-Control Optimization of Large Space Structures," Paper presented at NASA Symposium in Recent Experiences in Multidisciplinary Analysis and Optimization, April 1984.

[8]Salama, M., Hamidi, M., and Demsetz, L., "Optimization of Controlled Structures," *Proceedings of the Workshop on Identification and Control of Flexible Space Structures*, Jet Propulsion Laboratory (JPL) Publication 85-29, JPL, Pasadena, CA, April 1, 1985, Vol. 2, pp. 311–327.

[9]Khot, N. S., Eastep, F. E., and Venkayya, V. B., "Optimal Structural Modifications to Enhance the Optimal Active Vibration Control of Large Flexible Structures," *Proceedings of the 26th AIAA/ASME/ASCE/AHS Structures, Structural Dynamics and Materials Conference*, AIAA, Washington, DC, April 1985, pp. 134–142.

[10]Hale, A. L., Lisowski, R. J., and Dahl, W. E., "Optimal Simultaneous Structural and Control Design of Maneuvering Flexible Spacecraft," *Journal of Guidance, Control and Dynamics*, Vol. 8, Jan-Feb. 1985, pp. 86–93.

[11]Bodden, D. S. and Junkins, J. L., "Eigenvalue Optimization Algorithms for Structure/Controller Design Iterations," *Journal of Guidance, Control and Dynamics*, Vol. 8, Nov-Dec. 1985, pp. 697–706.

[12]Junkins, J. L. and Bodden, D. S., "A Unified Approach to Structure and Control System Design Iterations," Paper presented at Fourth International Conference on Applied Numerical Modeling, Tainan, Taiwan, Dec. 1984.

[13]Junkins, J. L. and Rew, D. W., "A Simultaneous Structure/Controller Design Iteration Method," *Proceedings of the 4th American Control Conference*, American Automatic Control Council, Boston, MA, 1985.

[14]Gustafson, C. L., Aswani, M., Doran, A. L., and Tseng, G. T., "ISAAC (Integrated Structural Analysis and Control) Via Continuum Modeling and Distributed Frequency Domain Design Techniques," *Proceedings of the Workshop on Identification and Control of Flexible Space Structures*, Jet Propulsion Laboratory, Pasadena, CA, JPL 85-29, April 1985, pp. 287–310.

[15]Elliott, L. E., Mingori, D. L., and Iwens, R. P., "Performance of Robust Output Feedback Controller for Flexible Spacecraft," *Proceedings of the Second VPI & SU/AIAA Conference on Dynamics and Control of Large Flexible Spacecraft*, AIAA Astrodynamics Technical Committee, Blacksburg, VA, June 1979, pp. 409–420.

[16]Canavin, J. R., "The Control of Spacecraft Vibrations Using Multivariable Output Feedback," AIAA Paper 78-1419, Aug. 1978.

[17]Balas, M. J., "Direct Output Feedback Control of Large Space Structures," *Journal of the Astronautical Sciences*, Vol. XXVII, No. 2, April-June 1979, pp. 157–180.

[18]Brogan, W. L., *Modern Control Theory*, 2nd ed., Prentice-Hall, Englewood Cliffs, NJ, 1985, Chap. 16.

[19]Lust, R. V., "Control Augmented Structural Synthesis," Ph.D. Dissertation, University of California, Los Angeles, 1986.

[20]Schmit, L. A. and Farshi, B., "Some Approximation Concepts for Efficient Structural Synthesis," *AIAA Journal*, Vol. 12, May 1974, pp. 692–699.

[21]Schmit, L. A. and Miura, H., "Approximation Concepts for Efficient Structural Synthesis," NASA CR 2552, March 1976.

[22]Lust, R. V. and Schmit, L. A., "Alternative Approximation Concepts for Space Frame Synthesis," *AIAA Journal*, Vol. 24, Oct. 1986, pp. 1676–1684.

[23]Soosar, K. et al., "Passive and Active Suppression of Vibration Response in Precision Structures—State-of-the-Art Assessment," Charles Stark Draper Laboratories, Inc., Cambridge, MA, Tech. Rept. R-1138, Vol. 2, Feb. 1978.

[24]Hurty, W. C. and Rubinstein, M. F., *Dynamics of Structures*, Prentice-Hall, Englewood Cliffs, NJ, 1964.

[25]Starnes, J. H. Jr. and Haftka, R. T., "Preliminary Design of Composite Wings for Buckling, Stress and Displacement Constraints," *Journal of Aircraft*, Vol. 16, Aug. 1979, pp. 564–570.

[26]Haftka, R. T. and Kamat, M. P., *Elements of Structural Optimization*, Martinus-Nijhoff, Boston, MA, 1985, Chap 6.

[27]Schmit, L. A. and Miura, H., "A New Structural Synthesis Capability—ACCESS 1," *AIAA Journal*, Vol. 14, May 1976, pp. 661–671.

[28]Vanderplaats, G. N., "CONMIN—A Fortran Program for Constrained Function Minimizatoin," NASA TM X-62,282, Aug. 1973.

[29]Fleury, C. and Braibant, V., "Structural Optimization—A New Dual Method Using Mixed Variables," University of Liege, Belgium, LTAS Rept. SA-115, March 1984.

[30]Horner, G. C. and Walz, J. E., "A Design Technique for Determining Actuator Gains in Spacecraft Vibration Control," *Proceedings of the 26th AIAA/ASME/ASCE/AHS Structures, Structural Dynamics and Materials Conference*, AIAA, Washington, DC, April 1985, pp. 143–151.